Benchmark of the HYMAGYC code

G. Fogaccia , S. Briguglio, G. Vlad

Associazione EURATOM-ENEA, Frascati, (Rome) Italy

The HYMAGYC code (HYbrid MAgnetohydrodynamics GYrokinetic Code) is composed by a MHD module interfaced with a particle-in-cell gyrokinetic module, suitable to study energetic particle driven Alfvénic modes in general high pressure axisymmetric equilibria, with perturbed electromagnetic fields fully retained. The MHD module solves resistive MHD linear equations including the kinetic response of the energetic particles in the momentum conservation equation, through the divergence of their pressure tensor. It is an initial-value version of the original eigenvalue MHD stability code MARS [1] and is adapted for the computation of the perturbed scalar potential $\delta\phi$ and the perturbed vector potential $\delta\vec{A}$. The gyrokinetic module, in turn, evolves gyrocentre phase-space coordinates of the energetic particles in the fluctuating fields according to the nonlinear gyrokinetic equations of motion [2] and yields the energetic particle pressure tensor back to the MHD solver, closing the single step iteration loop. A flux coordinate system (s, χ, φ) is used, with s the normalized radial flux coordinate proportional to the square root of the poloidal flux function, χ the generalized poloidal angle and φ the toroidal one.

Gyrocentre equations of motion are expanded up to order $O(\varepsilon^2)$ and $O(\varepsilon\varepsilon_B)$, where $\varepsilon \approx \rho_H/L_n$ is the gyrokinetic ordering parameter (with ρ_H being the energetic ion Larmor radius and L_n the equilibrium density scale length) and $\varepsilon_B \approx \rho_H/L_B < \varepsilon$ (with L_B being the equilibrium magnetic field scale length). The gyrokinetic ordering $k_\perp \rho_H \approx 1$, $e_H\delta\phi/T_H \approx e_H|\delta\vec{A}|/(m_H \mathrm{v}_H c) \approx \varepsilon$ is assumed (with $k_\perp$ the perpendicular, to the equilibrium magnetic field, wave vector of the fluctuating fields, e_H, m_H, T_H, v_H the charge, mass, temperature and thermal velocity of energetic species).

As a first step, the gyrokinetic module has been tested with respect to the single particle orbits in the magnetic equilibrium fields. Typical energetic particle unperturbed orbits projected in the poloidal cross section are shown in Fig. 1.

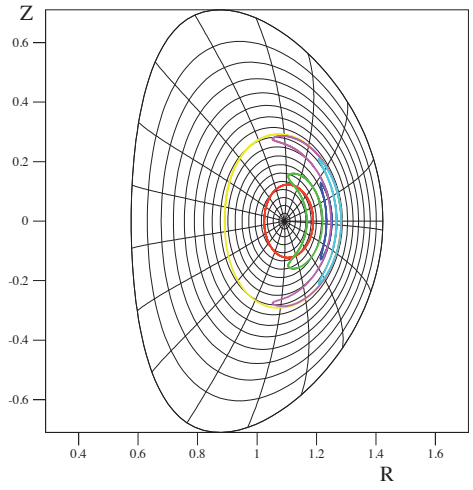

Figure 1: Energetic particle unperturbed orbits in the (R,Z) plane.

In order to test the energetic particles response, the gyrokinetic module has been tested by supplying assigned electromagnetic fields as functions of time and space. Suitable limits have been considered in order to develop a reference analytical

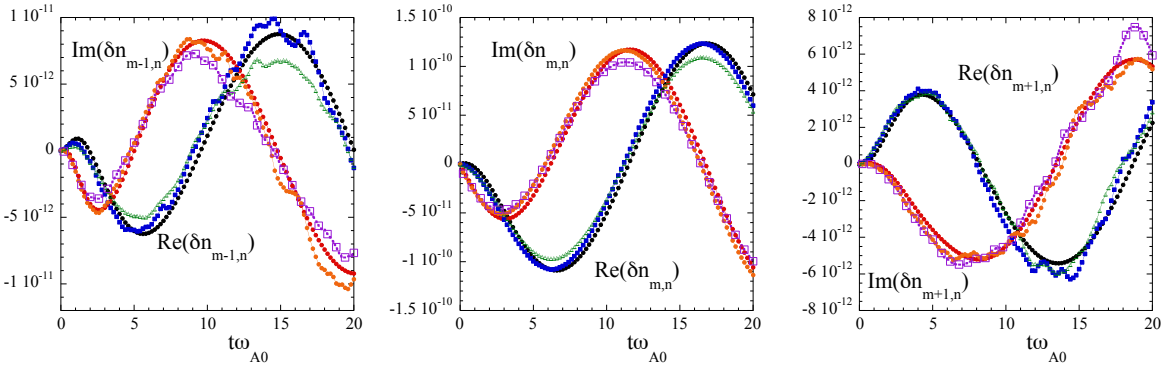

Figure 2: Fourier components of energetic particle perturbed density vs time, at $s = 0.5$, for $n = m = 4$, aspect ratio $R_0/a = 100$, $\rho_{H0}/a = 0.001$, $v_{H0}/v_{A0} = 0.1$, $T_{H\perp}/T_{H\parallel} = 0.01$ and $\omega/\omega_{A0} = (0.3 + i0.01)$ with ρ_{H0} and v_{H0} being the on-axis Larmor radius and thermal velocity of the energetic particle, and v_{A0} and ω_{A0} the on-axis Alfvén velocity and frequency.

model: large aspect ratio R_0/a (R_0 and a being the major and minor plasma radius), circular magnetic flux surfaces, flat safety factor q profile, circulating energetic particles with $\rho_H/a \ll 1$, unperturbed particle motion, no mirroring term in the parallel velocity equation, linearized Vlasov equation for the energetic particle distribution function, relaxation term of the energetic particle initial non-equilibrium distribution function in the Vlasov equation turned off, $|\delta\vec{A}_\perp| \ll \delta A_\parallel$ (with $\delta\vec{A}_\perp$ and $\delta A_\parallel$ the perpendicular and parallel perturbed vector potential). This benchmark has also been extended to the gyrokinetic module of the HMGC code [3] which evolves energetic particles in the guiding-center approximation $k_\perp\rho_H \ll 1$, large aspect ratio, circular shifted magnetic flux surfaces and $\delta\vec{A}_\perp = 0$. A bi-Maxwellian distribution function has been assumed as initial energetic particle distribution function, with $T_{H\perp}/T_{H\parallel} \to 0$ (with $T_{H\perp}$ and $T_{H\parallel}$ the perpendicular and parallel energetic ion temperature, respectively); a single Fourier component for the e.m. fields $\delta\phi_{m,n}$ and $\delta A_{\parallel,m,n}$ has been used (with m and n the poloidal and toroidal mode numbers, respectively), with a bell-shaped radial profile and time dependence $\propto e^{-i\omega t}$. In Fig. 2, the perturbed components $(m-1,n)$ (left), (m,n) (center) and $(m+1,n)$ (right) of the (normalized) energetic particle density are shown, for the analytical model (black and red curves), for the HYMAGYC kinetic module (blue and orange) and for the HMGC one (green and pink). The agreement of HYMAGYC results with the analitycal and HMGC ones is good: energetic particle perturbed density has a (m,n) dominant component, the $(m-1,n)$, $(m+1,n)$ satellites are more noisy and smaller by one order of magnitude.

Then, some of the analytical model constraints have been relaxed: mirroring term in the parallel velocity equation, perturbed linear terms in the particle coordinate evolution equations and relaxation term of the energetic particle initial distribution function in the Vlasov equation

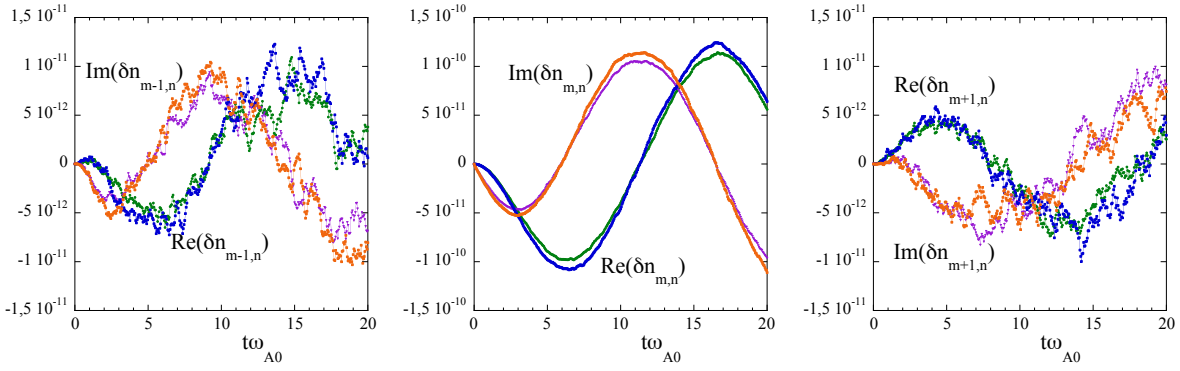

Figure 3: Fourier components of energetic particle perturbed density vs time. Curve colors are the same used in Fig. 2: blue and orange for HYMAGYC results, green and pink for HMGC ones.

have been turned on. The comparison is then performed between the gyrokinetic modules of HYMAGYC and HMGC (see Fig. 3), for the same energetic distribution function and parameters used in the previous example. The $(m-1,n)$, $(m+1,n)$ components are more noisy than those of the analitycal case (Fig. 2 left and right), but a good agreement between HMGC and HYMAGYC results is again obtained.

Finally, the HYMAGYC gyrokinetic module has been interfaced with the MHD one: the energetic particle pressure tensor, computed by the gyrokinetic module, is returned to the solver of MHD equations, thus providing a selfconsistent simulation. Using HYMAGYC in the same limit of validity of HMGC, the benchmark case has been performed using an equilibrium (generated by CHEASE [4]) corresponding to a circular poloidal cross section with $R_0/a = 10$, a monotonic safety factor q profile varying from $q_0 = 1.1$ on axis to $q_1 = 1.9$ at the plasma edge. Perturbations with $n = 2$, $m = 1,2,3,4$, and an energetic ion population described by a Maxwellian, with $\rho_{H0}/a = 0.01$ and $v_{H0}/v_{A0} = 1.0$ are assumed. Similar phenomenology is shown by the two codes. At low energetic particles equilibrium density, $n_{H0}/n_{i0} \lesssim 0.002$, ($n_{H0}$ and n_{i0} being the on axis values of energetic particle and thermal ion densities), the most unstable mode is located in the upper Alfvén continuum (Fig. 4), while, at higher density values, the most unstable mode lays in the lower Alfvén continuum (Fig. 5). In Figs. 4, 5 the power spectrums of the perturbed scalar potential are shown in the plane $(s,\omega/\omega_{A0})$

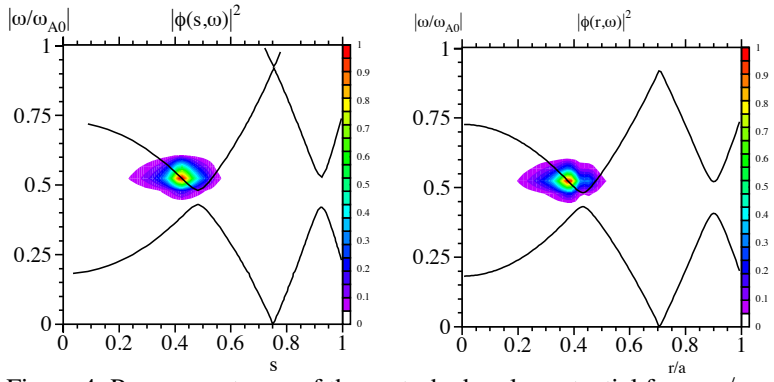

Figure 4: Power spectrums of the perturbed scalar potential for $n_{H0}/n_{i0} = 0.00175$, $v_{H0}/v_{A0} = 1.0$ and $\rho_{H0}/a = 0.01$: HYMAGYC code (left), HMGC code (right).

for HYMAGYC results (left), and in the plane $(r/a,\ \omega/\omega_{A0})$ for HMGC ones (right), with r the radial coordinate in quasi cylindrical coordinate system. Note that for the present equilibrium $r/a \approx s$. In Fig. 6, the growth rates (left) and real frequencies (center) of the unstable modes obtained by HMGC and HYMAGYC are shown, as the on axis energetic particle density is varied, while in Fig. 6 (right) the growth rates versus v_{H0}/v_{A0} for a fixed value $\beta_{H0} \simeq 0.007$ (corresponding to the case with $n_{H0}/n_{i0} = 0.00175$ in Fig. 6 left) are reported. For low values of energetic particle density, the frequencies and growth rates of the upper continuum unstable mode are similar between HYMAGYC and HMGC; for higher values of energetic particle density, a larger discrepancy both in frequency and growth rate is observed for the lower continuum unstable mode.

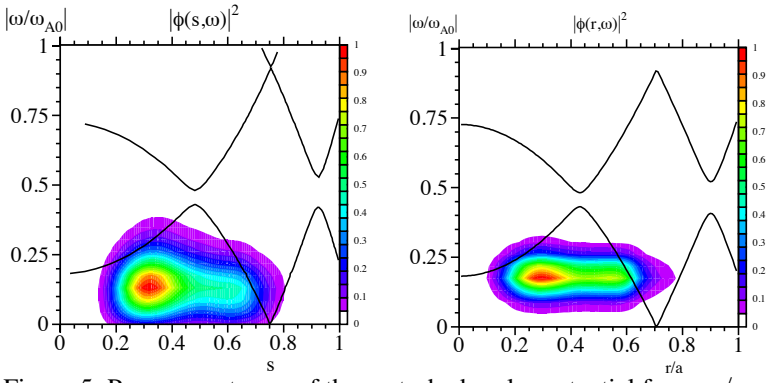

Figure 5: Power spectrums of the perturbed scalar potential for $n_{H0}/n_{i0} = 0.00375$, $v_{H0}/v_{A0} = 1.0$ and $\rho_{H0}/a = 0.01$: HYMAGYC code (left), HMGC code (right).

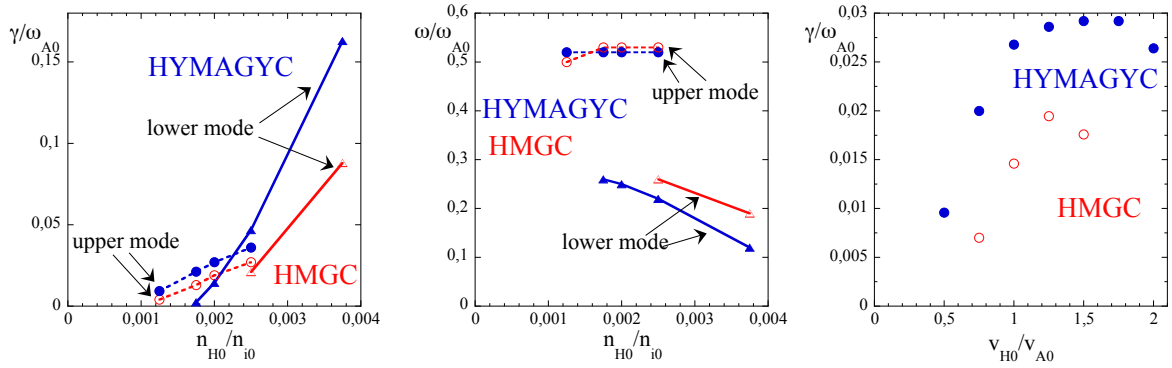

Figure 6: Normalized growth rates (left) and frequencies (center) versus n_{H0}/n_{i0} ($v_{H0}/v_{A0} = 1.0$); normalized growth rates versus v_{H0}/v_{A0} (right) ($\beta_{H0} \simeq 0.007$). HMGC (red open symbols), HYMAGYC (blue full symbols).

References

[1] A. Bondeson, G. Vlad and H. Lütjens. IAEA Technical Committee Meeting on Advances in Simulations and Modelling of Thermonuclear Plasmas, Montreal, 1992, pg 306, Vienna, Austria, 1993. International Atomic Energy Agency.

[2] A.J. Brizard and T.S. Hahm, Reviews of Modern Physics, **79** (2007)

[3] S. Briguglio, G. Vlad, F. Zonca and C. Kar, Physics of Plasmas, **2** (1995)

[4] H. Lütjens, A. Bondeson and O. Sauter, Comput. Phys. Commun. **95** (1996) 47

This work, supported by the European Communities under the contract of Association between EURATOM and ENEA was partially carried out within the framework of the Task Force on Integrated Tokamak Modelling of the European Fusion Development Agreement. The views and opinions expressed herein do not necessarily reflect those of the European Commission.